

# Simulation Model of a SiC Power MOSFET Variables Estimation and Control of a Power Source

E Baghaz, N M'asirdi, K Frifita, A Naamane, M Boussak

## ► To cite this version:

E Baghaz, N M'asirdi, K Frifita, A Naamane, M Boussak. Simulation Model of a SiC Power MOSFET Variables Estimation and Control of a Power Source. ICINCO 2017- International Conference on Informatics in Control, Automation and Robotics, Jul 2017, madrid, Spain. hal-01966868

**HAL Id: hal-01966868**

**<https://hal-amu.archives-ouvertes.fr/hal-01966868>**

Submitted on 30 Dec 2018

**HAL** is a multi-disciplinary open access archive for the deposit and dissemination of scientific research documents, whether they are published or not. The documents may come from teaching and research institutions in France or abroad, or from public or private research centers.

L'archive ouverte pluridisciplinaire **HAL**, est destinée au dépôt et à la diffusion de documents scientifiques de niveau recherche, publiés ou non, émanant des établissements d'enseignement et de recherche français ou étrangers, des laboratoires publics ou privés.

# Simulation Model of a SiC Power MOSFET

## *Variables Estimation and Control of a Power Source*

E. Baghaz, N.K. M'Sirdi, K. Frifita, A. Naamane and M. Boussak

*Aix Marseille Université, CNRS, ENSAM, Université de Toulon, LSIS UMR 7296, 13397, Marseille France*

*LSIS UMR 7296 and HyRES Lab, RMEI*

*nacer.msirdi@Lsis.org*

**Keywords:** Electro-thermal Model, boost DC/DC converter, Power source, SiC MOSFET Behavior, Estimation and control

**Abstract:** An electro-thermal model of a power SiC MOSFET is proposed. The thermal model, is coupled with the physical model through the interaction between the transistor power loss and the junction temperature. For validation of this model, the simulation curves are compared to the manufacturer's experimental curves. As first application, a boost DC/DC converter is considered. An observer is proposed to estimate the MOSFET voltage  $V_{DS}$ , the power and the junction temperature. These estimates are used to control the converter. The proposed model and estimator give sufficiently good temperature and power estimation. The Power source obtained using DC/DC converter is efficient, allowing the power loss reduction and robust.

## 1 INTRODUCTION

SiC MOSFET devices have a wide operation ranges in voltage, current and temperatures, then the knowledge of their characteristics and disposal of a good model become necessary. As wide as is the model validity domain, more and more high can be the control precision to achieve a high efficiency (Maxim and Maxim, 1999; Pushpakaran et al., 2015). A simple analytical PSpice model for SiCMOSFET have been proposed for high power modules in (Johannesson and Nawaz, 2016). In this paper we are interested by the SiC MOSFET C2M0025120D CREE (1200V, 90A), when operating at very high frequencies.

The MOSFET device characteristics can be extracted from manufacturer's experimental curves (data sheets). Simulations are very important in electric systems design as well as for mechatronics case study. Prototyping is necessary for the optimization of power electronic circuits. To get realistic simulations and accurate results, we need good and precise models for an operating domain as wide as possible (Leonardi et al., 1997).

The models proposed in the well known simulation softwares like Psim, Pspice, LMS AMESIM, Saber and other are often limited in their precision, field of application or complexity. The most of them are piece-wise linear. They are very, often valid only in a restricted area and must be completed using the components Data Sheet. To get reliable re-

sults based on simulations, we need accurate models, with acceptable precision. The precision of these models are very often limited to some operational points or region. The devices may be, in some applications, used in very wide operation ranges (Bejoy et al., 2015a)(Bejoy et al., 2015b).

In this paper, we propose an electro-thermal behavior model of a Silicon Carbide MOSFET (SiC). The electrical behavior sub-model is based on the well known EKV MOSFET Model (see (Enz et al., 1987)). Then a thermal dissipation model, expressed like Resistance-Capacitance (RC) Foster network, is coupled to the electrical model. The lost power contributes to the heating of the MOSFET internal junction. The heat transfer is described by a Foster electrical equivalent network.

For validation of this model, the simulation curves are compared to the manufacturer's experimental data (curves of data sheets).

The efficiency of the PhotoVoltaic (PV) system, obtained using this DC/DC converter and the proposed control, is robust against temperature variation. When Temperature varies from 25°C to 150°C, the PV system efficiency is reduced globally by only 4%. The SiC MOSFET power loss is analyzed to reduce its effect on the PV source efficiency.

## 2 SiC MOSFET BASED SOURCE

## 2.1 System description

As a first application using this SiC MOSFET model, we consider an energy source (PV panel) connected through a boost DC/DC converter driven by an analog MPPT based control, with as load a 50Ω resistance. This device is used to control a PV panel (PV S75), see figure (2.1). The proposed control system is analog to avoid the use of a computer based architecture.

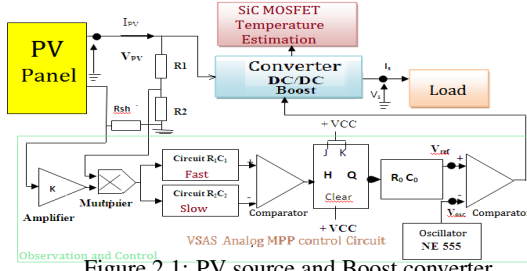


Figure 2.1: PV source and Boost converter

We have developed an analog circuit which estimates, on the fly, the needed MOSFET voltage, the power dissipated and the Junction temperature.

## 2.2 DC/DC conversion with a SiC MOSFET

In DC/DC converters, the most important power loss is due to the ON and OFF switching transition. The losses are proportional to the switching frequency and the values of the parasitic capacitances of power MOSFET component. So the characteristics of the SiC MOSFET used for commutation are of main importance (Time of response,  $R_{ds(on)}$ , ...).

The efficiency of the PV system depends on the used power converter and the control robustness against temperature variations and perturbations. When Temperature varies from 25°C to 150°C, the PV system efficiency is reduced and the system characteristics are perturbed.

This led us to choose a recently proposed SiC MOSFET which can operate under high frequencies and temperature condition. The SiC MOSFET, C2M0025120D, proposed by CREE is studied and used in a PV system (Figure 2.1 and 2.2) which is composed by:

- PV panel SP75 which can generate a voltage  $V_{PV}=13V$  a current  $I_{PV}=4.2A$  and a power  $P_{PV}=55W$
- DC/DC Boost using the SiC MOSFET proposed by CREE: C2M0025120D, operating at a control frequency  $f=10kHz$  (Figure 2.2),
- a Schottky diode C3D04060,
- an analog circuit used to estimate the MOSFET junction temperature, as proposed in this paper,
- an analog circuit proposed for the MPPT control,
- The system load is resistance  $R_L=50\Omega$ .

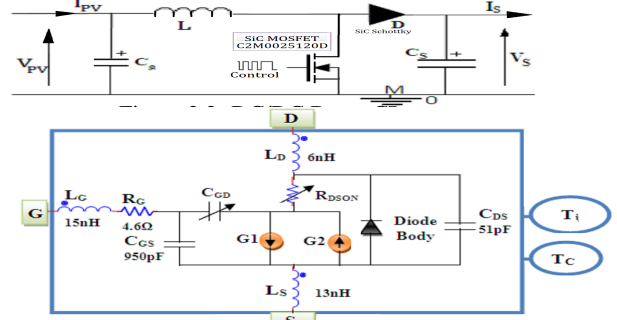


Figure 3.1: Model of a SiC MOSFET

## 3 DYNAMIC MODEL

The model is developed for the SiC MOSFET and is included to PSpice simulation software library. The electrothermal behavior of SiC MOSFET is analyzed, modeled and simulated under PSpice software.

### 3.1 SiC MOSFET component model

In a DC/DC converter the most important component is the MOSFET which is subject to the perturbations and thermal effect. Switching transition at high frequency (to control the input and output signals) lead to power dissipation and heating of the system. Thermal flux propagation will then impact the circuit behaviour. This is mainly due to the signals distortions (PWM) and parasitic impedance. A good behavior model is needed to describe the MOSFET dynamics.

#### 3.1.1 SiC MOSFET Electric Model

In figure 3.1, we present the model we have developed for and implemented under Pspice, to simulate the SiC MOSFET C2M0025120D proposed by CREE. Note that this model is more precise, with regard to the LTspice model proposed by the manufacturer CREE (Bejoy et al., 2015b) (Bejoy et al., 2015a), as it is composed by 2 switched current sources.

In addition it takes into account package parasitic inductances ( $L_G, L_D, L_S$ ) connected to the gate, drain, source and resistances ( $R_G, R_{DS(on)}$ ). The inductances and resistances allow description of power losses in commutations. The resistance  $R_G$  describes the Gate power losses in high frequencies operation.

$\alpha$  and  $n$  define the triode region and  $\lambda$  is the length of the MOSFET conduction channel. The gate threshold voltage is noted  $V_{th}$ .

The output current  $I_{DS} = I_{G1} - I_{G2}$  (Enz et al., 1987). The MOSFET equations ( $V_{DS}, I_{DS}, R_{ds(on)}, V_{GS} \dots$ ) are the following

$$I_{DS} = I_{G1}(V_p - V_s) - I_{G2}(V_p - V_D) \quad (1)$$

$$I_{G1} = I_S * (Ln(1 + exp(\frac{V_p - V_s}{2U_T}))^2 \quad (2)$$

$$I_{G2} = I_S * (\ln(1 + \exp \frac{V_p - V_D}{2U_T}))^2 \quad (3)$$

Where  $V_S$ ,  $V_G$ ,  $V_D$  are the source, gate and drain voltages of the MOSFET, respectively.  $V_p = \frac{(V_G - U_T)}{K_s}$  is the pinch-off voltage and  $I_S = 2 * U_T^2 * K_s * g_m$  is the specific current ( $g_m$  is a trans-conductance and  $K_s$  a slope factor). The model equations are in function of the MOSFET junction temperature.  $U_T$  is the thermodynamic voltage.

### 3.1.2 Thermal Model

To describe the thermal behavior, expressing that the power losses are dissipated heating the MOSFET junction which has thermal exchanges with the case and the component environment, we consider a Foster's  $RC$  network. We use 14  $RC$  cells to describe the thermal coupling. The junction and case temperatures  $T_j$  and  $T_c$  are related through the thermal impedance  $Z_{TH}$  and depend on the power losses  $P_{Perte}$  (see figure 3.2).

$$T_j = T_c + P_{Perte} * Z_{TH} \quad (4)$$

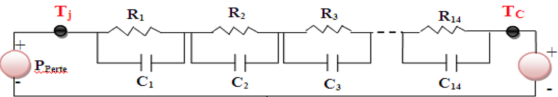
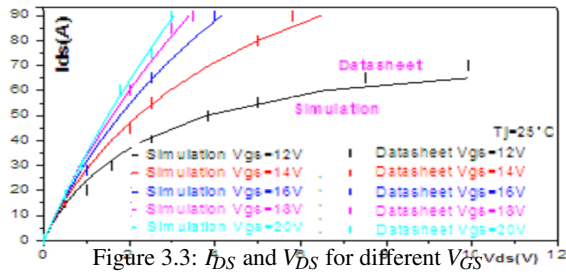
$$Z_{TH} = \sum_{i=1}^{14} R_i * (1 - \exp \frac{-t}{R_i C_i})$$


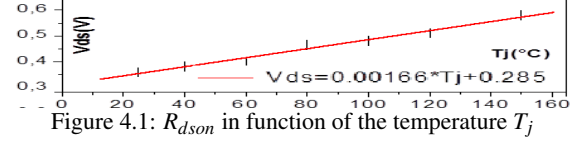
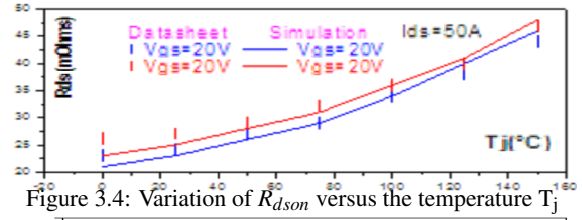
Figure 3.2: Thermal propagation model

## 3.2 Simulations and Model Validation

The developed model has been implemented in Saber, Pspice, Psim and Matlab softwares and compared to the experimental curves presented by the SiC MOSFET data sheet for its validation (Mudholkar et al., 2015). The figure 3.3 compares the Drain-Source current ( $I_{ds}$ ) versus the MOSFET output voltage ( $V_{DS}$ ) for several Gate-Source voltages ( $V_{GS}$ ) under a temperature of 25°C. Simulation results (continuous lines) are in good agreement with the data sheet values (bars).



- For  $V_{GS}$  values less than 4V, the MOSFET is not controlled because the threshold voltage  $V_{th}$  is not reached. When the MOSFET start operation  $V_{GS} > V_{th} > 4V$ , and then the current  $I_{DS}$  increases gradually with  $V_{GS}$ . The results are in good agreement.



The figure 3.4 shows the simulated and the actual Drain-Source resistance ( $R_{ds(on)}$ ) in function of the temperature variation for a current equal to  $I_{DS}=50A$  and voltage  $V_{GS}=20V$ . The obtained curves are very close in a wide temperature range (up to  $T=150^\circ C$ ).

In conclusion, the proposed electrothermal model is very accurate and able to describe the dynamic behavior of the SiC MOSFET with a very good precision.

## 4 ESTIMATION AND CONTROL

### 4.1 Observer for variables estimation

As seen in figure 3.5 the variation of the resistance  $R_{DSon}$  in function of the temperature  $T_j$  can be approximated by the following equation:

$$R_{DSon}(T_j) = R_{DSon}(300^\circ K) \left(1 + \frac{\alpha}{100}\right)^{(T_j - 300)} \quad (5)$$

$$V_{DS} = \zeta \cdot (R_{DSon}(T_j)) \cdot I_D$$

Let us introduce the variable  $\zeta$  to account for the variable structure feature of the system.  $\zeta = 0$  means that the MOSFET is off and  $\zeta = 1$  means that it is on. The junction temperature  $T_j$  grows with the MOSFET output voltage  $V_{DS}$  and power losses. In the figure 4.1, we note that the relation between  $V_{DS}$  and  $T_j$  is almost linear.

For parameters estimation and variables observation we can consider a first order (linear) regression model, during the period where the MOSFET is on. The solid line (in red) of the figure ?? confirms, from the simulations and data sheet experiments, the good precision of this approximation. Thus we can write.

$$V_{DS} = A * T_j + B \quad (6)$$

From the simulation result of figure 4.1, we can deduce by estimation that  $A = 0.001666$  and  $B = 0.285$  and then we can consider to estimate the junction temperature in average by  $T_j = (V_{DS} - B)/A$ .

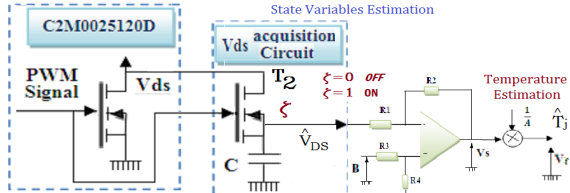


Figure 4.2: Estimation of the state Variables

#### 4.1.1 Estimation of Electric variables

The subsystem model is obvious if we take  $P = V.I$  as output and the current and voltage as inputs. Let us consider the estimations of the PV panel voltage  $\hat{V}_{PV}$  and current  $\hat{I}_{PV}$ . These estimations are implemented in the circuit of figure (2.1). The small shunt resistor  $R_{sh}$  gives us an image of the current by the voltage  $V_r$  and an image of the PV voltage is produced by the bridge of resistances  $R_1$  and  $R_2$ .

$$\begin{aligned} V_r &= a_1 \cdot \hat{I}_{KV} = I_{PV} * R_{sh} \\ V_p &= a_2 \cdot \hat{V}_{PV} = \frac{R_2}{R_1 + R_2} * V_{PV} \end{aligned} \quad (7)$$

The estimation of the instantaneous PV power is needed for the control, at two time instants  $t_1$  and  $t_2$ , in order to estimate its gradient. We can then deduce, using a signal multiplier, the produced PV power by  $\hat{P} = \hat{V}_{PV} \cdot \hat{I}_{PV}$ .

It remains now to estimate the power difference between two time instants. This can be done through two different time delays circuits  $\tau_1 = R_1 C_1$  and  $\tau_2 = R_2 C_2$  to get the delayed power estimations  $\hat{P}_1$  and  $\hat{P}_2$  and their difference  $\Delta P = \hat{P}_1 - \hat{P}_2$ , using a signal comparison component.

#### 4.1.2 Observer for Temperature Estimation

The Drain-Source voltage ( $V_{DS}$ ) must be estimated when the MOSFET turns ON ( $\zeta = 1$  means that the MOSFET state is ON). To get, in practice, the variable  $\zeta$  which account for the MOSFET state we use an additional MOSFET ( $T_2$ ) connected to the Gate and the Drain of the previous MOSFET. As shown in figure 4.2,  $T_2$  is controlled by the same PWM signal and receives the voltage  $V_{DS}$ .

Its source is connected to a capacitance  $C$  to which it transmits the voltage  $v = \zeta \cdot V_{DS}$ . Then the MOSFET  $T_2$  controls the charge of the capacitance  $C$ , under the voltage  $V_{DS}$  (when it is ON  $\zeta = 1$ ). When the capacitance is charged, the voltage will reach the value  $\hat{V}_{DS}$ , as an estimation of the Drain-Source voltage  $V_{DS}$ . Its discharge will be slow as it is connected to an Operational Amplifier, in the other side (when  $\zeta = 0$ ). Then it will keep the estimation  $\hat{V}_{DS}$ .

The next estimations are obviously produced by an inverse-amplifier (defined with the resistances  $R_1, R_2, R_3$  and  $R_4$ ) and a signal multiplier to get

$$V_s = \hat{V}_{DS} - B \quad \text{and} \quad V_f = \hat{T}_j = \frac{1}{A} V_s = T_j \quad (8)$$

Then we are able to develop analog estimations of the voltages  $\hat{V}_{PV}$ , and  $\hat{V}_{DS}$ , current  $\hat{I}_{PV}$ , the power  $\hat{P}_1$  at  $t - \tau_1$  and  $\hat{P}_2$  at  $t - \tau_2$  and their difference  $\Delta P = \hat{P}_1 - \hat{P}_2$ , with in addition the temperature  $\hat{T}_j$ .

## 4.2 Control Circuit (MPPT)

The behavior of the conversion systems of this kind of renewable energy is VSAS (Variable Structure Automatic Systems) and highly dependent on variations in climate parameters, such as temperature and irradiation. The MPPT algorithms are expected to maximize, **at each time instant**, the produced power. Several techniques have been designed to search this optimal MPP. In figure 2.1, we propose an analog circuit which produces the MPPT control signal as given by the algorithms developed in our previous work ((M' Sirdi et al., 2014)).

If the PV panel power increases or decreases ( $\Delta P \geq 0$  or  $\Delta P \leq 0$ ), the JK Flip-Flop state changes correspondingly. The flip-flop output  $Q$  is used to produce a triangular signal ( $V_{ref}$  as a reference for commutation) and then the PWM required for the MOSFET control. The reference signal frequency is fixed to 10kHz, by means of the choice of  $\tau_0 = R_0 C_0$  the integrator time constant.  $V_{ref}$  allows to adjust the duty factor.

## 4.3 Simulation results and discussion

### 4.3.1 The PV control System simulation

The PV system, described in section 2, plus the estimation and control circuits of section 4, are simulated under the physical modeling oriented software Pspice.

The irradiation is considered, for the first simulation, fixed at  $100W/m^2$  with the temperature  $T_j = 25^\circ C$ . The proposed control generates a good PWM signal with a duty factor 0.7. In the same figure 4.3-F1 and F2 show the voltage and current of the PV panel in green ( $V_{PV}, I_{PV}$ ) and the outputs of the DC/DC converter ( $V_s, I_s$ ).

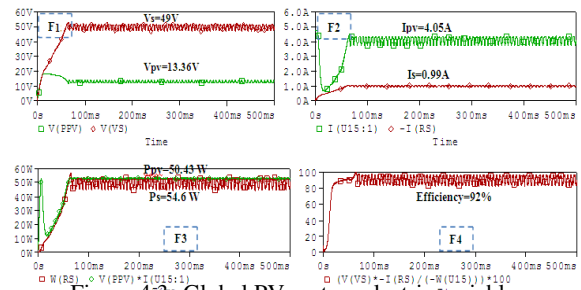


Figure 4.3: Global PV system electric variables

The PV output voltage is  $V_{PV} = 13.36V$ . The DC/DC output voltage is  $V_s = 49V > V_{PV}$ , and the current is  $I_s = 0.99A < I_{PV} = 4.05A$ .

The figure 4.3-F3 shows that the PV output power  $P_{pv} = 54,6W$  (in green) is practically completely transmitted by the DC/DC converter to the load  $P_s = 50,43W$  (in red). The instantaneous powers ( $P_{pv}$ ,  $P_s$ ) oscillate in the neighborhood of the Maximum Power Point (F3 and F4). The global PV system has an efficiency equal to  $\eta = 92\%$  (see figure 4.3-F4). In figure 4.3-F1 (respectively F2) we show the voltages (currents) at converter input DC/DC Boost  $V_{PV}$  ( $I_{PV}$  in green) and output  $V_s$  ( $I_s$  in red). Figure 4.3-F4 shows the overall performance of the PV system.

The PWM signal produced by our control MPPT circuit allows us to retrieve the MOSFET state (On/Off) giving a very good estimation of the information signal  $\zeta$ . This signal is important for the estimation of  $V_{DS}$ . It allows us to distinguish the period where the MOSFET (C2M0025120D) is OFF and when it is ON. When the MOSFET state is ON  $\zeta = 1$ , the estimated voltage  $\hat{V}_{DS}$  converges to the MOSFET one  $V_{DS}$ . When the state MOSFET is OFF  $\zeta = 0$ , the second MOSFET T2 is also OFF (as it receives the same PWM signal). The estimated voltage  $\hat{V}_{DS}$  is kept, more or less, constant by the capacitance C.

This proves the efficiency of the proposed SASV MPPT control algorithm combined whit the proposed estimation circuits.

#### 4.3.2 Thermal behavior and temperature estimation

Simulations have been done for different values of the studied MOSFET junction temperature going from 25°C up to 110°C. The estimated temperatures are presented in table 1. We can remark than the maximum error is 3°C.

$T_j$ MOSFET SiC °C	Estimated (°C)
25	25
30	31
40	39
50	47
75	72
100	100
110	112

Table 1: The estimated temperatures

The estimated voltage is  $V_{DS} = 320mV$  (see figure 4.4-F1 in green), The voltage  $V_{ds}$  acquired (in Figure 4.4-F2 in red) equals the average value of actual the voltage  $V_{ds}$  of the investigated transistor, during his On state (see figure 4.6-F2 in green), justifying good  $V_{ds}$  earned value. The output voltage of the amplifier of figure 4.2 Subtractor is 40mV order (Figure 4.4-F3), which shows that the constant B in equation 6 equals 280mV. Finally F4 compares the MOSFET

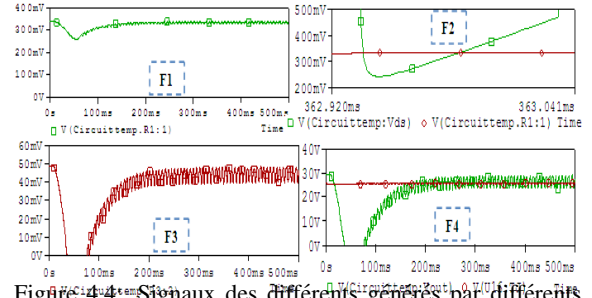


Figure 4.4: Signaux des différents blocs de circuit de température

Temperature C2M0025120D	Efficiency of PV system
25°C	92%
50°C	90%
75°C	89.93%
100°C	88.9%
125°C	88.5%
150°C	88%

Table 2: Influence of Temperature on efficiency

temperature  $T_j$  (in green) to its estimation given by the thermal model (in red).

The investigated transistor temperature is of the order of 25.45 °C (Figure 4.6-F4), in other words, the transistor switches under a room temperature, which confirms the good functioning of the overall PV system. Temperature issued by the circuit developed during this work is identical with that given by the thermal model of the MOSFET in figure 2, with a difference less than 0.2 °C.

#### 4.3.3 Power losses in the PV system

As already mentioned DC/DC power converters suffer from loss of power loss due to components heating. In this context, we have studied the influence of the temperature on the MOSFET Characteristics.

The table2 summarizes the results obtained when the junction temperature increases from 25 °C to 150 °C. The system performance decreases of 4%. Which shows that the monitoring of the MOSFET temperature, in a power converter is necessary to reduce power losses.

In order to show performance degradations when the MOSFET is poorly controlled (deformation of the PWM signal), we compare the simulation results in figure 4.8 to the normal situation (when the MOSFET is controlled by a PWM signal without deformation Figure 4.3-F1). F1 shows a distorted signal of PWM and F2 the junction temperature.

Note that this study was conducted on the same PV system, under the same climate conditions, namely a 1000W/m<sup>2</sup> irradiance and a temperature of 25°C. When the MOSFET of the DC/DC Boost converter is controlled by a deformed PWM signal (Figure 4.5-F1), its temperature rises to 30°C (Figure F2)



instead of 25°C in normal operation case (Figure 4.3 F4). That is to say a temperature increase of 16.66% leads to the overall performance from 92% (during normal operation) down to 73.8% (Figure 4.8-F3). This represents a decline of efficiency of 18.2%.

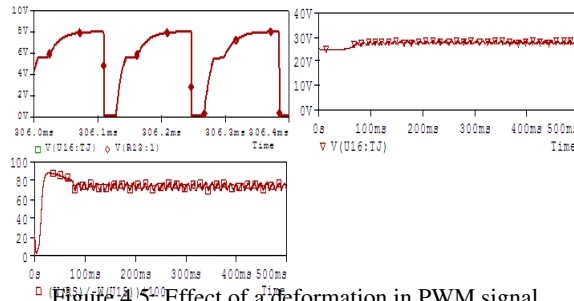


Figure 4.5: Effect of a deformation in PWM signal

## 5 CONCLUSIONS

An electro-thermal model of a power SiC MOSFET is proposed for efficient circuits simulation. This model describes the links of the various physical parameters of the MOSFET ( $V_{ds}$ ,  $I_{ds}$ ,  $T_j$ ...), which clarify the electrical and thermal coupling. This allows to get more realistic simulations. To validate the proposed model equations and parameters, we have compared simulation results with those of datasheet of the MOSFET. It appears that the electro-thermal model has high accuracy even in high temperatures and high voltages.

Then, we have developed a circuit that gives measures and estimates of the system state variables and the junction temperature of the MOSFET. The comparison of the temperature of the thermal model of the MOSFET with that of the developed estimation circuit shows that there is a good agreement. In order to show the good convergence of the estimates, we have used this power component in a DC/DC Boost converter for adaptation between a PV source and a 50Ω resistive load.

The converter is controlled by an analog MPPT control proven to be efficient, fast and robust. Then we have studied the influence of the temperature on the overall performance of the same PV system. It appears that by varying the temperature of the junction of the transistor from 25 °C to 150 °C, the overall performance of the PV system decreases by 4%. In the same work, we consider also the effect of deformation on the PWM signal and we show how the system performance degrades.

The PV system with DC/DC converter control is investigated using Pspice. The results show that the proposed model is the most precise compared to all the literature existing models. An analog circuit observer is then implemented. The control based on the

observer estimations is also implemented as an analog circuit. This model can be used for simulation of any application using this SiC MOSFET into Pspice software. The simulation results show that the proposed model is efficient, reliable and show that our electro-thermal model approach and the proposed estimator give good temperature estimation and control.

## Acknowledgements

This research activity is held by the SASV group of the LSIS and funded by the BPI in a FUI projects. Special acknowledgements are addressed to all our project partners.

## REFERENCES

- Bejoy, N., Pushpakaran, N., Stephen, B., Bayne, B., Wang, G., and Mookken, J. (2015a). Fast and accurate electro-thermal behavioral model of a commercial sic 1200v, 80 mohm power mosfet. *IEEE Transactions on Electron Devices*.
- Bejoy, N., Pushpakaran, N., Stephen, B., Bayne, B., Wang, G., and Mookken, J. (2015b). A simple approach on junction temperature estimation for sic mosfet dynamic operations within safe operating area. *IEEE Transactions on Electron Devices*, 12.
- Enz, C., Krummenacher, F., and Vittoz, E. (1987). A cmos chopper amplifier. *IEEE Journal of Solid-State Circuits*, 22.
- Johannesson, D. and Nawaz, M. (2016). Analytical pspice model for sic mosfet based high power modules. *Microelectronics Journal*, 53:167–176. QC 20170410.
- Leonardi, C., Raciti, A., Frisina, F., and Letor, R. (1997). A new pspice power mosfet model with temperature dependent parameters: evaluation of performances and comparison with available models. *Thirty-Second Conference Record of the 1997 IEEE IAS Annual Meeting, IAS97*.
- Maxim, A. and Maxim, G. (1999). A high accuracy power mosfet spice behavioral macromodel including the device selfheating and safe operating area simulation. *40th APEC Dallas*.
- M'Sirdi, N., Nehme, B., Abarkan, M., and Rabbi, A. (2014). The best mppt algorithms by vsas approach for renewable energy sources (res). In *EFEA 2014*, pages 1–7, Paris France.
- Mudholkar, M., Ahmed, S., Ericson, M., Frank, S. S., Britton, C. L., and Mantooth, H. A. (2015). Datasheet driven silicon carbide power mosfet model. *IEEE Transactions on Power Electronics*.
- Pushpakaran, B., Bayne, S., Wang, G., and Mookken, J. (2015). Fast and accurate electro-thermal behavioral model of a commercial sic 1200v 80 mohms. *IEEE Pulsed Power Conference (PPC)*.